Slow exciton spin relaxation in single self-assembled $In_{1-x}Ga_xAs/GaAs$ quantum dots

Hai Wei, Guang-Can Guo, and Lixin He*

Key Laboratory of Quantum Information, University of Science and Technology of China, Hefei 230026, People's Republic of China and Synergetic Innovation Center of Quantum Information and Quantum Physics, University of Science and Technology of China, Hefei 230026, People's Republic of China

(Received 9 October 2013; revised manuscript received 28 May 2014; published 16 June 2014)

We calculate the acoustic phonon-assisted exciton spin relaxation via spin-orbit coupling in single self-assembled $In_{1-x}Ga_xAs/GaAs$ quantum dots using an atomistic empirical pseudopotential method. We show that the transition rate from bright to dark exciton states is zero under Hartree-Fock approximation. The exciton spin relaxation time obtained from sophisticated configuration interaction calculations is approximately 15–55 μs in pure InAs/GaAs QDs and even longer in alloy dots. These results are more than three orders of magnitude longer than previous theoretical and experimental results (a few ns), but agree with more recent experiments which suggest that excitons have long spin-relaxation times (>1 μs).

DOI: 10.1103/PhysRevB.89.245305 PACS number(s): 72.25.Rb, 71.70.Ej, 73.21.La

I. INTRODUCTION

Self-assembled quantum dots (QDs) have many attractive features as fundamental building blocks for quantum information processing. Huge progress has been made experimentally in the initialization, manipulation, and readout of the electron (hole) spins in quantum dots in the last decade. However, the short electron/hole spin lifetime is still a major obstacle for such applications. There have been extensive studies of single electron and hole spin relaxation in QDs caused by hyperfine interaction with nuclear spins [1–6] and the spin-phonon interaction due to spin-orbit coupling (SOC) [7–16]. However, exciton spin relaxation has been less commonly studied.

Excitons and biexcitons in QDs have been used to generate single photons [17] or entangled photon pairs [18]. Bright and dark excitons have also been proposed as possible quantum bits (qubits) [19,20]. The fast nonradiative relaxation of bright excitons limits the maximal single-photon device emission rate and thus lowers the source efficiency [21]. This property also lowers the quality of the single photons and the fidelity of the entangled photon pairs generated by biexciton cascade decay [22]. Understanding the mechanism of exciton spin relaxation is therefore of fundamental importance. However, despite its importance, spin relaxation in excitons is still not well understood and full of controversy.

Exciton spin relaxation has been measured by several groups in different types of QDs [23–25]. The measured spin relaxation time ranges from 200 ps [23] to 167 ns [24]. The spin-relaxation time calculated from perturbation theory is approximately 2 ns in In(Ga)As/GaAs QDs at 4 K [26], which seems to be in good agreement with some experimental values [25]. All of these studies suggest fast spin relaxation for excitons. However, recent direct measurements [27,28] of dark exciton lifetimes show that dark excitons actually have rather long lifetimes ($\sim$1.5 μs), which serve as a lower bound for exciton spin relaxation, in sharp contrast to previous results.

To solve the controversy, we calculate the first-order phonon-assisted exciton spin relaxation in single self-assembled $In_{1-x}Ga_xAs/GaAs$ QDs using an atomistic empirical pseudopotential method (EPM) [29]. Remarkably, we find that in the Hartree-Fork (HF) approximation, the transition from a bright to dark state is forbidden. Sophisticated configuration interaction (CI) [30] calculations suggest that the bright-to-dark exciton transition is approximately tens of μs in InAs/GaAs QDs, much longer than previous calculations [26] and early experimental values [23–25] but supported by more recent measurements [27].

This paper is organized as follows. In Sec. II, we introduce the methods we used to calculate the exciton spin-relaxation time. In Sec. III, we present and discuss the calculated spin lifetimes in typical self-assembled $In_{1-x}Ga_xAs/GaAs$ QDs. We summarize in Sec. IV.

II. METHODS

A. Exciton spin relaxation

Figure 1 depicts the typical energy levels of an exciton in $In_{1-x}Ga_xAs/GaAs$ QDs. The electron-hole exchange interaction [31] splits the ground neutral exciton (X) states into two nearly degenerate doublets accordingly to their total angular momentum of the exciton $M = J_h + s$, where $J_h = 3/2$ and $s = 1/2$ are the angular momentum of the hole and the electron respectively. At two lower levels, in which the electron and hole have the same spin directions, the total angular momentum of the excitons is $|M| = 2$. The excitons cannot couple to the light field, and are therefore called dark excitons. In contrast, at two upper levels, in which the electron and hole have the opposite spin directions, $|M| = 1$. The excitons are optically active and are called bright excitons. Single-dot spectroscopy shows that the typical energy space between bright and dark states, Δ_{BD}, is approximately 100–300 μeV [32], caused by the electron-hole exchange interaction. Because of the asymmetry of the exchange interaction [32–34], the bright (dark) states further split into two sublevels B_1 and B_2 (D_1 and D_2), as schematically shown in Fig. 1. The energy splitting between B_1 and B_2, known as fine-structure splitting (FSS), is usually a few tens of μeV [32,34].

The electron and hole spin-phonon interaction due to SOC can cause spin flip [7,8,12–14]. For excitons, such spin flip results in a transition from a bright to dark exciton and the emission of a phonon or vice versa (see Fig. 1).

*helx@ustc.edu.cn

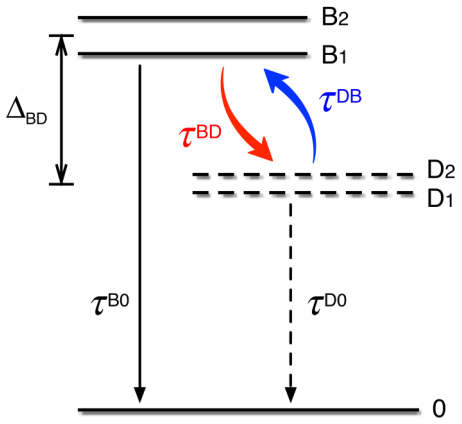

FIG. 1. (Color online) Schematic depiction of exciton spin relaxation. B_1 and B_2 (D_1 and D_2) are the two sublevels of bright (dark) state. τ^{BD} (τ^{DB}) is the transition time from bright (dark) to dark (bright) states. τ^{B0} (τ^{D0}) is the radiative decay time of the bright (dark) excitons. Δ_{BD} is the exchange splitting between bright and dark excitons.

The Hamiltonian for excitons with the exciton-phonon interaction reads

$$H = H_0^X + \sum_\nu H_\nu^{X-ph}, \tag{1}$$

where H_0^X is the Hamiltonian for excitons. H_ν^{X-ph} describes the electron/hole-phonon interactions [35],

$$H_\nu^{X-ph} = \sum_{c,v,\mathbf{q}} \left[\alpha_\nu^e(\mathbf{q}) a_c^\dagger a_c + \alpha_\nu^h(\mathbf{q}) a_v^\dagger a_v\right] \times e^{i\mathbf{q}\cdot\mathbf{r}}\left(b_{\nu,\mathbf{q}} + b_{\nu,-\mathbf{q}}^\dagger\right), \tag{2}$$

where a ($a^\dagger$) denotes the annihilation (creation) operator of the electron in the conduction (c) or valence (v) band, and b_ν ($b_\nu^\dagger$) is the annihilation (creation) operator of νth phonon modes. $\alpha_\nu^e(\mathbf{q})$ [$\alpha_\nu^h(\mathbf{q})$] is the electron(hole)-phonon-coupling strength.

In the presence of spin-orbit coupling, the electron/hole-phonon interaction results in spin-up and spin-down mixture, and therefore causes electron/hole spin flip, which ultimately leads to exciton spin relaxation. The exciton spin-relaxation rate from a bright (B) to a dark (D) state is given by the first-order Fermi's "golden rule" [26]:

$$\frac{1}{\tau_\nu^{BD}} = \frac{2\pi}{\hbar} \sum_{\mathbf{q}} \left|M_\nu^{BD}(\mathbf{q})\right|^2 (N_{\nu,\mathbf{q}} + 1)\delta(\Delta_{BD} - \hbar\omega_{\nu,\mathbf{q}}), \tag{3}$$

where $N_{\nu,\mathbf{q}} = (e^{\hbar\omega_{\nu,\mathbf{q}}/k_BT} - 1)^{-1}$ is the Bose-Einstein distribution function for phonons. $\hbar\omega_{\nu,\mathbf{q}}$ is the phonon energy, with $\omega_{\nu,\mathbf{q}} = c_\nu|\mathbf{q}|$, where c_ν is the speed of sound for the ν = LA (longitudinal-acoustic phonon) and TA (transverse-acoustic phonon) modes. $\mathbf{q}$ is the phonon wave vector. Because Δ_{BD} is very small, only acoustic phonons are involved in the process.

The exciton-phonon-coupling matrix is given by [35],

$$M_\nu^{BD}(\mathbf{q}) = \left\langle \Psi_X^D \middle| H_\nu^{X-ph} \middle| \Psi_X^B \right\rangle = \alpha_\nu^e(\mathbf{q}) \left\langle \Psi_X^D \middle| e^{i\mathbf{q}\cdot\mathbf{r_e}} \middle| \Psi_X^B \right\rangle - \alpha_\nu^h(\mathbf{q}) \left\langle \Psi_X^D \middle| e^{i\mathbf{q}\cdot\mathbf{r_h}} \middle| \Psi_X^B \right\rangle, \tag{4}$$

where Ψ_X^B (Ψ_X^D) are the bright (dark) exciton wave functions. We have considered three electron/hole-phonon interaction mechanisms in QDs [7,14], including the interaction due to (i) the deformation potential (ν = LADP), (ii) the piezoelectric field for the longitudinal modes (ν = LAPZ), and (iii) the piezoelectric field for the transverse modes (ν = TAPZ). Details of $\alpha_\nu^e(\mathbf{q})$, $\alpha_\nu^h(\mathbf{q})$ and related parameters can be found in Ref. [14]. The overall spin relaxation time from bright to dark states, T_1, is

$$1/T_1 = \sum_\nu \sum_B \sum_D 1/\tau_\nu^{BD}. \tag{5}$$

B. Empirical pseudopotential method

It is essential to have high-quality exciton wave functions to obtain accurate exciton spin relaxation times [14]. In this work, we use EPM to calculate single-particle energy and wave functions [29]. This method has been successfully applied to study the electronic and optical properties of self-assembled $In_{1-x}Ga_xAs/GaAs$ QDs [36]. We simulate lens-shaped $In_{1-x}Ga_xAs/GaAs$ QDs, grown along the [001] direction and embedded in a cubic GaAs matrix containing $60a_0 \times 60a_0 \times 60a_0$ eight-atom unit cells, where a_0 = 5.65 (Å) is the GaAs lattice constant. All atom positions $\{\mathbf{R}_{n,\alpha}\}$ (αth atom at site n) are optimized using the valence force field (VFF) method. [37] We obtain the electron and hole energy levels and wave functions by solving the single-particle Schrödinger equation,

$$\left[-\frac{1}{2}\nabla^2 + V_{\text{epm}}(\mathbf{r})\right]\psi_i(\mathbf{r}) = \epsilon_i\psi_i(\mathbf{r}), \tag{6}$$

where $V_{\text{epm}}(\mathbf{r}) = \sum_{n,\alpha} \hat{v}_\alpha(\mathbf{r} - \mathbf{R}_{n,\alpha}) + V_{\text{SO}}$ is the total electron-ion potential as superposition of local screened atomistic pseudopotential $\hat{v}_\alpha(\mathbf{r})$ and nonlocal spin-orbit potential V_{SO}. The atomistic pseudopotentials [29] are fitted to all the physically important properties of the materials, including band energies at high-symmetry points, effective masses, strained band offsets, and hydrostatic and biaxial deformation potentials of individual band edges. Especially, the spin-orbit parameters are fitted to the spin-orbit bands splitting of bulk materials. [14] Once the parameters are determined, there are no free parameters for modeling the QDs. The method naturally includes the Rashba and Dresselhaus SOC in a "first-principles" manner.

The single-particle Schrödinger equation is solved by the linear combination of bulk bands (LCBB) method [38]. We use eight bands for both the electrons and holes that take the interband coupling into account, which is very important for electron/hole spin relaxation. A $6 \times 6 \times 16$ k mesh converges very well with the results [14,29]. We apply a very small magnetic field B_z = 1 mT along the [001] direction to break the spin degeneracy. The energy differences between the spin-up and spin-down states caused by the external magnetic field are less than 0.1 μeV, and do not change the final results of exciton spin relaxation. We also test B_z = 100 mT, and the changes in exciton spin relaxation time are very small.

The exciton wave functions are obtained via the CI method [30] by expanding them as linear combinations of Slater determinants. The αth ($\alpha = D_1, D_2, B_1, B_2$) exciton wave

function is written as

$$\Psi_X^{\alpha}(\mathbf{r_e},\mathbf{r_h}) = \sum_{v}^{N_v}\sum_{c}^{N_c} C_{v,c}^{\alpha}\Phi_{v,c}(\mathbf{r_e},\mathbf{r_h}), \tag{7}$$

where N_v and N_c are the numbers of valence and conduction states included in the expansion. The coefficients $\{C_{v,c}^{\alpha}\}$ as well as the exciton energies are obtained by diagonalizing the many-particle Hamiltonian in terms of the Slater determinants basis set $\{\Phi_{v,c}\}$. The exciton energies and wave functions are well converged using $N_v = 20$ and $N_c = 12$ (including spin) in our calculations.

Once we have obtained exciton wave functions, the exciton wave-function overlap in Eq. (4) can be calculated as

$$\left\langle \Psi_X^D \middle| e^{i\mathbf{q}\cdot\mathbf{r_e}} \middle| \Psi_X^B \right\rangle = \sum_{v}^{N_v}\sum_{c_i,c_f}^{N_c} \left(C_{v,c_f}^D\right)^* C_{v,c_i}^B \left\langle \psi_{c_f}^e \middle| e^{i\mathbf{q}\cdot\mathbf{r_e}} \middle| \psi_{c_i}^e \right\rangle, \tag{8}$$

and

$$\left\langle \Psi_X^D \middle| e^{i\mathbf{q}\cdot\mathbf{r_h}} \middle| \Psi_X^B \right\rangle = \sum_{v_i,v_f}^{N_v}\sum_{c}^{N_c} \left(C_{v_f,c}^D\right)^* C_{v_i,c}^B \left\langle \psi_{v_f}^h \middle| e^{i\mathbf{q}\cdot\mathbf{r_h}} \middle| \psi_{v_i}^h \right\rangle, \tag{9}$$

where ψ_c^e (ψ_v^h) is the cth (vth) electron (hole) wave function [14].

The single-particle matrix elements, $\langle \psi_{c_f}^e | e^{i\mathbf{q}\cdot\mathbf{r_e}} | \psi_{c_i}^e \rangle$, are calculated in the Bloch basis of bulk InAs at the Γ point [14]. The bright (dark) exciton wave functions are dominated by configurations in which electron and hole have the opposite (same) pseudospin. The mixture of the configurations, in which electron and hole have the same (opposite) pseudospin because of heavy-hole–light-hole mixing, is rather small. Therefore, the matrix elements in Eq. (8) are expected to be very small because, if electrons $\psi_{c_i}^e$ and $\psi_{c_f}^e$ have the same pseudospins, in which $|\langle \psi_{c_f}^e | e^{i\mathbf{q}\cdot\mathbf{r_e}} | \psi_{c_i}^e \rangle|$ is large ($\sim$1), $|(C_{v,c_f}^D)^* C_{v,c_i}^B|$ is small ($<$0.01). On the other hand, if electrons $\psi_{c_i}^e$ and $\psi_{c_f}^e$ have opposite pseudospins, in which $|(C_{v,c_f}^D)^* C_{v,c_i}^B|$ is large ($\sim$0.5), the single-particle wave function overlaps, $|\langle \psi_{c_f}^e | e^{i\mathbf{q}\cdot\mathbf{r_e}} | \psi_{c_i}^e \rangle|$, must be very small [14]. The same arguments also apply to the holes.

III. RESULTS AND DISCUSSION

A. Hatree-Fork approximation

We start with the simplest case, using only the lowest electron and hole ($N_v = N_c = 2$) states to construct the exciton wave functions, which is equivalent to the HF approximation. Surprisingly, we find that the exciton spin-relaxation rate is zero in this approximation. To understand this result, we examine Eqs. (8) and (9) under the HF approximation in greater detail. We first examine the electron part of the exciton wave-function overlap, Eq. (8). Under the HF approximation, Eq. (8) can be written as

$$\begin{aligned}\left\langle \Psi_X^D \middle| e^{i\mathbf{q}\cdot\mathbf{r_e}} \middle| \Psi_X^B \right\rangle_{HF} &= \xi_{11}\sum_{v=1,2}\left[\left(C_{v,1}^D\right)^* C_{v,1}^B + \left(C_{v,2}^D\right)^* C_{v,2}^B\right] \\ &+ \xi_{12}\sum_{v=1,2}\left(C_{v,1}^D\right)^* C_{v,2}^B \\ &+ \xi_{12}^*\sum_{v=1,2}\left(C_{v,2}^D\right)^* C_{v,1}^B, \end{aligned}\tag{10}$$

where $\xi_{11} = \langle \psi_1^e | e^{i\mathbf{q}\cdot\mathbf{r_e}} | \psi_1^e \rangle = \langle \psi_2^e | e^{i\mathbf{q}\cdot\mathbf{r_e}} | \psi_2^e \rangle$, and $\xi_{12} = \langle \psi_1^e | e^{i\mathbf{q}\cdot\mathbf{r_e}} | \psi_2^e \rangle$. ψ_1^e (ψ_2^e) are the electron spin-up (-down) wave functions of the lowest energy level. Because ψ_1^e and ψ_2^e are Kramers degenerate states that are related by time-reversal symmetry, it is easy to prove that $\xi_{12} = 0$. Furthermore, the bright (Ψ_X^B) and dark (Ψ_X^D) exciton states are orthogonal:

$$\left\langle \Psi_X^D \middle| \Psi_X^B \right\rangle_{HF} = \sum_{v=1,2}\left[\left(C_{v,1}^D\right)^* C_{v,1}^B + \left(C_{v,2}^D\right)^* C_{v,2}^B\right] = 0. \tag{11}$$

By substituting ξ_{12} and Eq. (11) into Eq. (10), we have the electron part of the exciton wave-function overlap, $\langle \Psi_X^D | e^{i\mathbf{q}\cdot\mathbf{r_e}} | \Psi_X^B \rangle_{HF} = 0$. For the same reason, the hole part of the exciton wave-function overlap is $\langle \Psi_X^D | e^{i\mathbf{q}\cdot\mathbf{r_h}} | \Psi_X^B \rangle_{HF} = 0$. Therefore, the exciton-phonon interaction matrix element, $M_v^{BD}(\mathbf{q}) = 0$, meaning the exciton spin-relaxation rate equals zero under the HF approximation. Because $\xi_{11} \sim 1$ is very large, a small unorthogonality of the exciton wave functions may cause huge errors in the calculated spin-relaxation time. As it is prohibited in the HF approximation, we need to go beyond the approximation and do CI calculations to obtain the correct relaxation time.

B. Configuration interaction calculations

The CI-calculated exciton relaxation times of pure InAs/GaAs QDs are approximately 15–55 μs. The spin-relaxation times of alloy QDs are even longer. The exciton spin-relaxation times are determined by three factors: (i) Δ_{BD}, which determines the phonon momentum $\mathbf{q}$ involved in the process. The smaller Δ_{BD} leads to a longer spin-relaxation time because of lower phonon density involved; (ii) the spin mixing in the electron and hole single-particle wave functions, which determines single-particle relaxation time; and (iii) the exciton CI coefficients $\{C_{v,c}^{\alpha}\}$. All three factors are strongly affected by the geometry and chemical composition of the QDs.

We calculate the exciton relaxation time of lens-shaped pure InAs/GaAs QDs as a function of base diameter (height) while keeping height (base diameter) constant at $T = 4.2$ K. The exciton spin-relaxation times as well as Δ_{BD} are given in Fig. 2 as black lines. The calculated Δ_{BD} distributes mostly between 100–300 μeV, which is in good agreement with experimental values [32]. For pure dots, when dot height increases from 2.0 to 5.5 nm, Δ_{BD} decreases from 330 to 90 μeV [Fig. 2(a)]. We find that the exciton spin-relaxation time is dominated by the hole spin flip. This is because the *atomistic* part of the hole wave function is p-like which has strong SOC, whereas that of electron is s-like, and has much weaker SOC. However, there are two major differences between the single hole spin flip [7,8,10–14] and hole spin flip in an exciton. First, for single hole spin flip, the energy splitting between the spin-up and spin-down states is determined by the applied magnetic field. Therefore, the spin-flip rate is very sensitive to the applied magnetic field. At very low magnetic field, the spin flip is dominated by the two-phonon processes [13,14]. In contrast, the dark-bright exciton states always have large energy-level splitting due to the electron-hole exchange interaction even in the absent of applied magnetic field. Second, unlike the single-particle cases, the hole relaxation in excitons is further affected by the many-particle effects (i.e., the CI coefficients). The decrease of Δ_{BD} tends to prolong the spin-relaxation time,

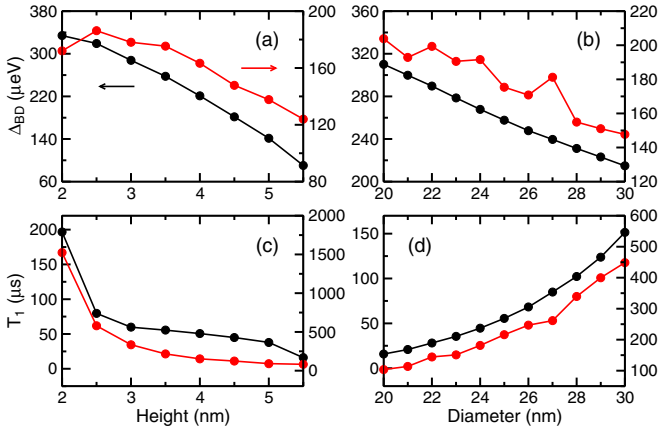

FIG. 2. (Color online) The upper panels show the exchange energy splitting between bright and dark states Δ_{BD} as functions of (a) dot height with dot diameter fixed at 25 nm and (b) dot diameter with dot height fixed at 3.5 nm. Corresponding exciton spin-relaxation times are shown in (c) and (d). Black lines are the results of pure InAs/GaAs QDs, whereas red lines are the results of $In_{0.7}Ga_{0.3}As$/GaAs QDs.

because less phonon is involved in the process. At the same time, the hole spin-flip time drops quickly with increasing dot height, because of the larger SOC effects [14]. These two factors compete with each other, and the overall effect is that the spin-flip time decreases first when dot height changes from 2.0 to 3.0 nm, reaching a relatively constant value as dot height further increases [Fig. 2(c)]. On the contrary, as the base diameter increases from 20 to 30 nm, Δ_{BD} decreases from 310 to 220 μeV [Fig. 2(b)], whereas increasing dot diameter also slows hole spin relaxation [14], and the exciton spin-relaxation time increases [Fig. 2(d)].

We also calculate the exciton spin-relaxation time of lens-shaped alloy $In_{0.7}Ga_{0.3}As$/GaAs QDs. The results are shown in Fig. 2 as red lines. These results are similar to those of pure QDs. The dark-bright splitting and spin-relaxation time of alloy QDs show some nonmonotonous behaviors as functions of dot height and dot diameter. This is due to the random distribution of In, Ga components in the alloy dot. Similar effects have been found on the single electron and hole relaxation time [14].

Generally, the exciton spin-relaxation time of alloy dots due to first-order spin-phonon coupling is much longer than that of the pure dots because alloy dots usually have smaller Δ_{BD}. In fact, exciton spin-relaxation time is very sensitive to Δ_{BD}, as demonstrated in Fig. 3. We compare the spin-relaxation times of two QDs. One QD is a lens-shaped InAs/GaAs dot with diameter $D = 20$ nm and height $h = 3.5$ nm. The other QD is an alloy dot with the same geometry but with Ga composition of $x = 0.3$. As we artificially change Δ_{BD}, the spin-relaxation times increase dramatically with decreasing Δ_{BD}, as $T_1 \sim \Delta_{BD}^{-\gamma}$, where $\gamma = 2.9$ for the pure dot and $\gamma = 2.3$ for the alloy dot from the numerical fitting.

The exciton dark-bright splitting Δ_{BD} also determines which mechanism is dominant for the spin flip. Figure 4 depicts the contributions of the three exciton-phonon interaction mechanisms to the total exciton spin-relaxation rate as a function of temperature. We take a lens-shaped InAs/GaAs

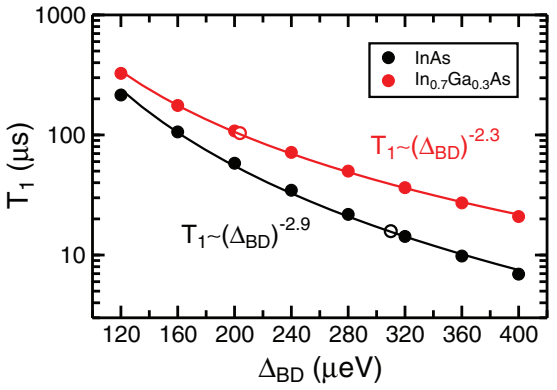

FIG. 3. (Color online) The change of exciton spin-relaxation times T_1 as we artificially vary Δ_{BD} in lens-shaped $In_{1-x}Ga_xAs$/GaAs QDs with base diameter $b = 20$ nm and height $h = 3.5$ nm. The open circles are results obtained by EPM, and the solid lines are fitted using $T_1 \sim \Delta_{BD}^{-\gamma}$.

QDs with base diameter $b = 20$ nm and height $h = 3.5$ nm as an example. The red, blue, and green line denote the LADP, LAPZ, and TAPZ contributions, respectively, whereas the black line is the total spin-relaxation rate. In the experimental temperature range (>4 K), the spin-relaxation rates from all mechanisms increase linearly with temperature, which is the signature of the first-order phonon processes. If we use $\Delta_{BD} = 310$ μeV, which is given by the EPM calculation, the LADP mechanism contributes the most to the total relaxation

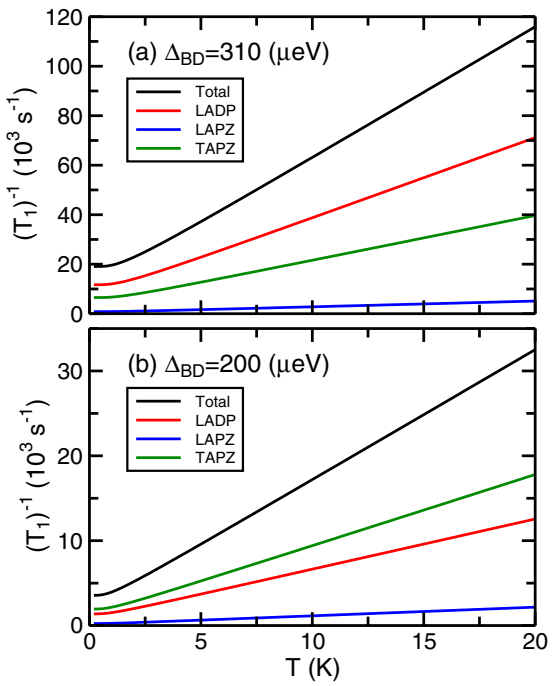

FIG. 4. (Color online) Exciton spin-relaxation rates of different mechanisms as a function of temperature in lens-shaped InAs/GaAs QDs with base diameter $b = 20$ nm and height $h = 3.5$ nm. The red, blue, and green lines denote the LADP, LAPZ, and TAPZ contributions, respectively. The black line is the total relaxation rate. (a) $\Delta_{BD} = 310$ μeV, and (b) $\Delta_{BD} = 200$ μeV.

rate, as shown in Fig. 4(a). However, if we (artificially) use a smaller $\Delta_{BD} = 200$ μeV, the TAPZ mechanism contributes the most, as shown in Fig. 4(b), because the exciton-phonon coupling strength $\alpha_{\mathrm{LADP}} \propto |\mathbf{q}|$, whereas $\alpha_{\mathrm{TAPZ}} \propto 1/|\mathbf{q}|$. Therefore a smaller Δ_{BD} makes the TAPZ mechanism dominant.

C. Discussion

Two exciton spin-relaxation mechanisms have been discussed in the literature, namely exchange interaction [39] and SOC [26]. In QDs smaller than the exciton Bohr radius, the exchange interaction is most significant in exciton spin relaxation, whereas the SOC mechanism dominates in the larger QDs studied here. The calculated spin-flip time is approximately 2 ns in the In(Ga)As/GaAs QDs at 4 K [26], which is a few orders of magnitude faster than that obtained in the present work. One possible reason is that in the previous calculations, the SOC were treated perturbatively. Cheng *et al.* have shown that, in the single-particle case, perturbation theory greatly overestimates the spin-relaxation rate [7]. The fast relaxation from perturbation theory is possibly due to the failure of the perturbation theory to ensure the orthogonality of both single-particle and many-particle wave functions. The (unorthogonal wave functions) approximation may not be a serious problem in other calculations; however, it is crucial in the present calculation as well as in the single-particle case. Because $\xi_{11} \gg \xi_{12}$, a small error in the orthogonality of the wave functions may cause large errors as discussed for the HF approximation above.

The exciton spin-relaxation time has been measured by several groups for different QDs. Kurtze *et al.* found that the spin-flip time is approximately 20 ns at 5 K and 1 ns at 110 K in In(Ga)As/GaAs QDs [25]. Snoke *et al.* found that the dark-to-bright exciton transition time is 200 ps at $T \approx 10$ K in InP QDs [23]. Johansen *et al.* found that the relaxation time is approximately 77–167 ns in In(Ga)As/GaAs QDs [24]. These experimental values seem to be in good agreement with previous theoretical results [26], all suggesting that the spin relaxation in excitons is very fast. However, in these experiments, spin-relaxation times were extracted from the bright exciton decay time, in which the exciton radiative decay ($\sim$1 ns) is much faster than the spin relaxation. Therefore, there might be very large errors in estimating the spin-relaxation time using bright exciton dynamics. A more accurate method to estimate the exciton spin-relaxation time is to measure the dark exciton lifetime which has extremely long radiative lifetime. Indeed, direct manipulation of dark exciton has recently become possible [27,28]. The measured dark exciton lifetime exceeds 1.5 μs at 5 K [27], which is the lower bound for the dark-to-bright exciton transition (note that at this temperature, $\tau^{BD}/\tau^{DB} \approx 1/2$), ruling out the fast spin relaxation in the exciton. This result is supported by the present calculations.

We would like to note that given the very long exciton relaxation time calculated here, the spin-relaxation time through a first-order spin-phonon interaction may not be the dominant mechanism for exciton spin relaxation. The roles of other mechanisms need to be further clarified, including hyperfine and second-order spin-phonon interactions. Nevertheless, the exciton spin-relaxation time should be much longer than previously reported, which favors quantum information processing.

IV. CONCLUSION

We present an atomistic pseudopotential calculation of the acoustic phonon-assisted exciton spin relaxation from bright to dark exciton in single self-assembled $In_{1-x}Ga_xAs/GaAs$ QDs. We show that the exciton spin-relaxation rate is zero under Hartree-Fock approximation. The spin-relaxation time calculated from sophisticated CI method is 15–55 μs in pure InAs/GaAs QDs and even longer in alloy dots, which is more than three orders of magnitude longer than previous theoretical and experimental results, but agrees with more recent experiments.

ACKNOWLEDGMENTS

L.H. acknowledges support from the Chinese National Fundamental Research Program 2011CB921200 and National Natural Science Funds for Distinguished Young Scholars.

[1] P.-F. Braun, X. Marie, L. Lombez, B. Urbaszek, T. Amand, P. Renucci, V. K. Kalevich, K. V. Kavokin, O. Krebs, P. Voisin, *et al.*, Phys. Rev. Lett. **94**, 116601 (2005).
[2] W. Yao, R.-B. Liu, and L. J. Sham, Phys. Rev. B **74**, 195301 (2006).
[3] M. Kroutvar, Y. Ducommun, D. Heiss, M. Bichler, D. Schuh, G. Abstreiter, and J. J. Finley, Nature (London) **432**, 81 (2004).
[4] Ł. Cywiński, Acta Phys. Pol. A **119**, 576 (2011).
[5] W. A. Coish and J. Baugh, Phys. Status Solidi B **246**, 2203 (2009).
[6] J. Fischer, W. A. Coish, D. V. Bulaev, and D. Loss, Phys. Rev. B **78**, 155329 (2008).
[7] J. L. Cheng, M. W. Wu, and C. Lü, Phys. Rev. B **69**, 115318 (2004).
[8] V. N. Golovach, A. Khaetskii, and D. Loss, Phys. Rev. Lett. **93**, 016601 (2004).
[9] M. Florescu and P. Hawrylak, Phys. Rev. B **73**, 045304 (2006).
[10] D. Heiss, S. Schaeck, H. Huebl, M. Bichler, G. Abstreiter, J. J. Finley, D. V. Bulaev, and D. Loss, Phys. Rev. B **76**, 241306(R) (2007).
[11] B. D. Gerardot, D. Brunner, P. A. Dalgarno, P. Öhberg, S. Seidl, M. Kroner, K. Karrai, N. G. Stoltz, P. M. Petroff, and R. J. Warburton, Nature (London) **451**, 441 (2008).
[12] A. V. Khaetskii and Y. V. Nazarov, Phys. Rev. B **64**, 125316 (2001).
[13] M. Trif, P. Simon, and D. Loss, Phys. Rev. Lett. **103**, 106601 (2009).

[14] H. Wei, M. Gong, G.-C. Guo, and L. He, Phys. Rev. B **85**, 045317 (2012).
[15] R. J. Warburton, Nat. Mater. **12**, 483 (2013).
[16] D. V. Bulaev and D. Loss, Phys. Rev. Lett. **95**, 076805 (2005).
[17] P. Michler, A. Kiraz, C. Becher, W. V. Schoenfeld, P. M. Petroff, L. Zhang, E. Hu, and A. Imamoglu, Science **290**, 2282 (2000).
[18] R. M. Stevenson, R. J. Young, P. Atkinson, K. Cooper, D. A. Ritchie, and A. J. Shields, Nature (London) **439**, 179 (2006).
[19] E. Biolatti, R. C. Iotti, P. Zanardi, and F. Rossi, Phys. Rev. Lett. **85**, 5647 (2000).
[20] A. Imamoğlu, D. D. Awschalom, G. Burkard, D. P. DiVincenzo, D. Loss, M. Sherwin, and A. Small, Phys. Rev. Lett. **83**, 4204 (1999).
[21] S. Strauf, N. G. Stoltz, M. T. Rakher, L. A. Coldren, P. M. Petroff, and D. Bouwmeester, Nat. Photon. **1**, 704 (2007).
[22] M. Reischle, G. J. Beirne, R. Roßbach, M. Jetter, and P. Michler, Phys. Rev. Lett. **101**, 146402 (2008).
[23] D. W. Snoke, J. Hübner, W. W. Ruhle, and M. Zundel, Phys. Rev. B **70**, 115329 (2004).
[24] J. Johansen, B. Julsgaard, S. Stobbe, J. M. Hvam, and P. Lodahl, Phys. Rev. B **81**, 081304(R) (2010).
[25] H. Kurtze, D. R. Yakovlev, D. Reuter, A. D. Wieck, and M. Bayer, Phys. Status Solidi C **8**, 1165 (2011).
[26] E. Tsitsishvili, R. v. Baltz, and H. Kalt, Phys. Rev. B **72**, 155333 (2005).
[27] J. McFarlane, P. A. Dalgarno, B. D. Gerardot, R. H. Hadfield, R. J. Warburton, K. Karrai, A. Badolato, and P. M. Petroff, Appl. Phys. Lett. **94**, 093113 (2009).
[28] E. Poem, Y. Kodriano, C. Tradonsky, N. H. Lindner, B. D. Gerardot, P. M. Petroff, and D. Gershoni, Nat. Phys. **6**, 993 (2010).
[29] A. J. Williamson, L.-W. Wang, and A. Zunger, Phys. Rev. B **62**, 12963 (2000).
[30] A. Franceschetti, H. Fu, L.-W. Wang, and A. Zunger, Phys. Rev. B **60**, 1819 (1999).
[31] A. Franceschetti, L. W. Wang, H. Fu, and A. Zunger, Phys. Rev. B **58**, R13367 (1998).
[32] M. Bayer, G. Ortner, O. Stern, A. Kuther, A. A. Gorbunov, A. Forchel, P. Hawrylak, S. Fafard, K. Hinzer, T. L. Reinecke, *et al.*, Phys. Rev. B **65**, 195315 (2002).
[33] G. Bester, S. Nair, and A. Zunger, Phys. Rev. B **67**, 161306(R) (2003).
[34] M. Gong, W. Zhang, G.-C. Guo, and L. He, Phys. Rev. Lett. **106**, 227401 (2011).
[35] T. Takagahara, Phys. Rev. B **60**, 2638 (1999).
[36] G. Bester, J. Phys: Condens. Matter **21**, 023202 (2009).
[37] P. N. Keating, Phys. Rev. **145**, 637 (1966).
[38] L.-W. Wang and A. Zunger, Phys. Rev. B **59**, 15806 (1999).
[39] E. Tsitsishvili, R. v. Baltz, and H. Kalt, Phys. Rev. B **67**, 205330 (2003).